Petroleum and Coal

Article **Open Access**

Estimation of Petroleum Reservoirs Geomechanical Parameters using Machine Learning Method

Mehdi Zallaghi [1], Malek Jalilian [2], Shahriar Fatemi [3], Amir H. Mohammadi [4]*

[1] *Tehran Petroleum Research Center, Petroleum University of Technology (PUT), Southern Sattarkhan St., Tehran, Iran*
[2] *Institute of Petroleum Engineering, School of Chemical Engineering, College of Engineering, University of Tehran, Tehran, Iran*
[3] *Namvaran Upstream Company, No.14, 4th Aseman St., Azadegan Highway, Chitgar, Tehran ,Iran*
[4] *Discipline of Chemical Engineering, School of Engineering, University of KwaZulu-Natal, Howard College Campus, King George V Avenue, Durban 4041, South Africa*

Received January 20, 2021; Accepted March 30, 2021

Abstract

Geomechanical characterization plays a critical role in drilling and production design. The traditional methods for estimation of mechanical rock properties, such as experimental techniques, are expensive and time-consuming. Hence, fast and accurate computing tools such as Artificial Neural Networks (ANN) should be developed for this purpose. This study aims to develop an efficient computational tool to estimate geomechanical parameters based on well logging data. We present a robust approach to calculate the borehole geomechanical parameters using a machine learning technique. The ANFIS approach is utilized to estimate the geomechanical parameters, such as Young's modulus, Poisson's ratio, bulk modulus, shear modulus, etc., based on well logging data. Two classes of the ANFIS approach, including C-mean and subtractive clustering algorithms, are applied to estimate rock elastic parameters. The comparison of the outcomes to conventional methods shows a reasonable estimation of these parameters with significant accuracy. Although there are slight differences between the accuracies of these two systems, this methodology is quite fast applying the inexpensive tool to determine the mechanical rock parameters.

Keywords: *Geomechanics; Well log; Parameter estimation; Neural-fuzzy system; Machine Learning; Petroleum drilling.*

1. Introduction

Recent studies have shown that Artificial Intelligence (AI) is an effective computational method, which has been mostly inspired by biological systems. AI is used in a wide range of tasks in different fields [1]. Two major applications of AI are data analysis and prediction [2]. Machine learning methods can be applied in seismic inversion, log analysis, 3D reservoir modeling, and geomechanical studies [3].

Stress state is a piece of vital knowledge in the oil and gas fields for safe drilling and production operations. Accurate estimation of the elastic parameters and pressure leads to a more reliable prediction of field behavior. Geomechanics is intertwined with rock characterization and mechanics [4]. Therefore, many correlations can be used to derive the dynamic and static rock properties and UCS. AI can help obtaining better results for rock elastic parameters to develop functional relationships for data and can provide a powerful toolbox for nonlinear and multidimensional interpolations [5].

The next step is estimating pore pressure at which the fluid is contained within the pore space of the rock at a specific depth [6]. The pore pressure is either reduced or increased during the production or injection of the hydrocarbon fluids. Due to the significant hydrocarbons production, and the consequent reservoir pressure decline, the overburden weight is successively transferred to the rock matrix and effective stress in the reservoir increases. The

growth of compressive stress can lead to reservoir compaction [7]. Many methods have been proposed to predict sandstone reservoir pore pressure using well-logs and seismic data, but there is no widely accepted technique for carbonate reservoirs [8].

Previous studies on the pore pressure prediction were made by Hottmann and Johnson derived from well log data for shale formations [9]. This approach is based on the deviation of the measured properties from the normal trend line. Afterward, many researchers have successfully used several logs, including resistivity, sonic transit time, porosity, and other well log data for pore pressure estimation [10].

Furthermore, wellbore instability is a common problem during drilling due to variations of stress concertation, causing casing collapse, lost circulation, etc. In order to avoid this issue, some phenomena such as induced fractures or breakouts need to be prevented by adjusting the stress with an appropriate mud weight window. There are many failure criteria for wellbore stability analysis, and Mohr-Coulomb is the most common method [11]. To obtain these criteria, accurate information about the rock's elastic parameters, pore pressure, and field stress is essential [12].

In this study, a machine learning method, namely Adaptive Network-based Fuzzy Inference System (Adaptive Neuro-Fuzzy Inference Systems: ANFIS), was applied to estimate the pore pressure, the rock elastic parameters, and the principal stresses in carbonate reservoirs in Iranian oil fields. Also, traditional correlation and ANFIS results were compared favorably, and the results were classified based on the best model. The database used in this study, consists of several different reports such as geophysics, geology, petrophysics, drilling, fracture study, zonation, static and dynamic modeling, and production. In each section, all data were analyzed and studied; however, comprehensive well log data were the most critical information comprised of the gamma-ray, density, and sonic logs that are fundamental for geomechanical modeling.

2. Methodology

Two approaches were used to estimate the geomechanical parameters, including conventional correlation and ANFIS methods. First, the elastic parameters were calculated, and then pore pressure was modeled based on the Eaton method and calibrated by the Modular Formation Dynamics Tester (MDT) test. Then, an ANFIS model was used to estimate these properties. The ANFIS is based on the Takagi–Sugeno fuzzy inference system. A wide range of data was required for borehole geomechanics.

2.1. Overburden stress

The upper layers' predominant heaviness can cause overburden or vertical stress (σ_v), which is one of the three principal stresses. Density-log used to estimate and analyze the cuttings at the surface can lead to a robust result. The vertical stress (σ_v) can be obtained using Eq. 1.

$$\sigma_V = g \int_0^h \rho(z)dz \quad (1)$$

where σ_v is the vertical stress; ρ (z) represents the bulk density at depth z; and g stands for the gravitational constant.

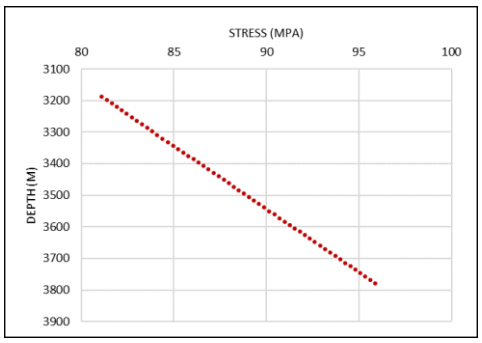

Figure 1. Overburden stress versus depth

The overburden stress was evaluated by deriving bulk density data. Figure 1 shows overburden stress as a function of depth. The trend of stress variation and well depth is linear and reaches 96 MPa in 3800 ft.

2.2. Elastic properties

Based on the available log data, it was recognized that shear wave velocity, one of the essential parameters, did not exist. Therefore, share delay time mode was calculated based on Greenberg and Castagna' relations. Figure 2 shows DT (us.ft) and calculated DTSM (us.ft) vs. depth (m). Shear-wave velocity can be estimated in brine-saturated composite lithology by a simple average of the arithmetic and harmonic means of the pure constituent lithology shear velocities as given by Eq. 2 [13]:

$$Vs = \frac{1}{2}\{[\sum_{i=1}^{L} x_i \sum_{j=0}^{Ni} a_{ij} v_p^j] + [\sum_{i=1}^{L} x_i (\sum_{j=0}^{Ni} a_{ij} v_p^j)^{-1}]^{-1}\} \quad (2)$$

$$\sum_{i=1}^{L} x_i = 1$$

where L is the number of pure mono-mineralic lithologic constituents; x_i represents the volume fraction of lithological constituent; a_{ij} stands for the empirical regression coefficients; *Ni* is the order of polynomial for constituent I; and v_P and v_S represent the P- and S-wave velocities (km.s), respectively.

There are several correlations to obtain the static elastic parameters from the dynamic parameters. The dynamic elastic rock parameters are converted to static based on Mordales and Marcinew and Bradford equations [14]. The geomechanical elastic parameters as function of depth were calculated from well log data, as shown in Figure 3.

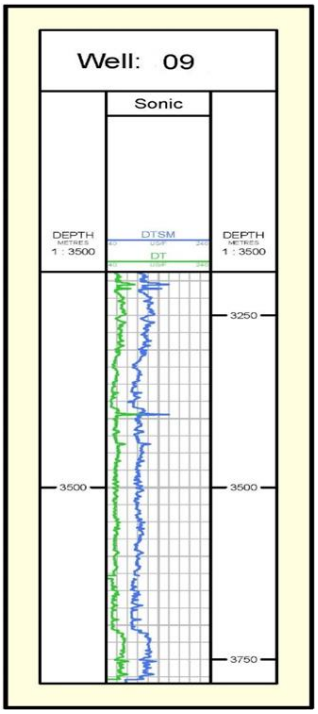

Figure. 2. Green line is DT (us/ft) and blue line is calculated DTSM (us/ft) vs. depth (m)

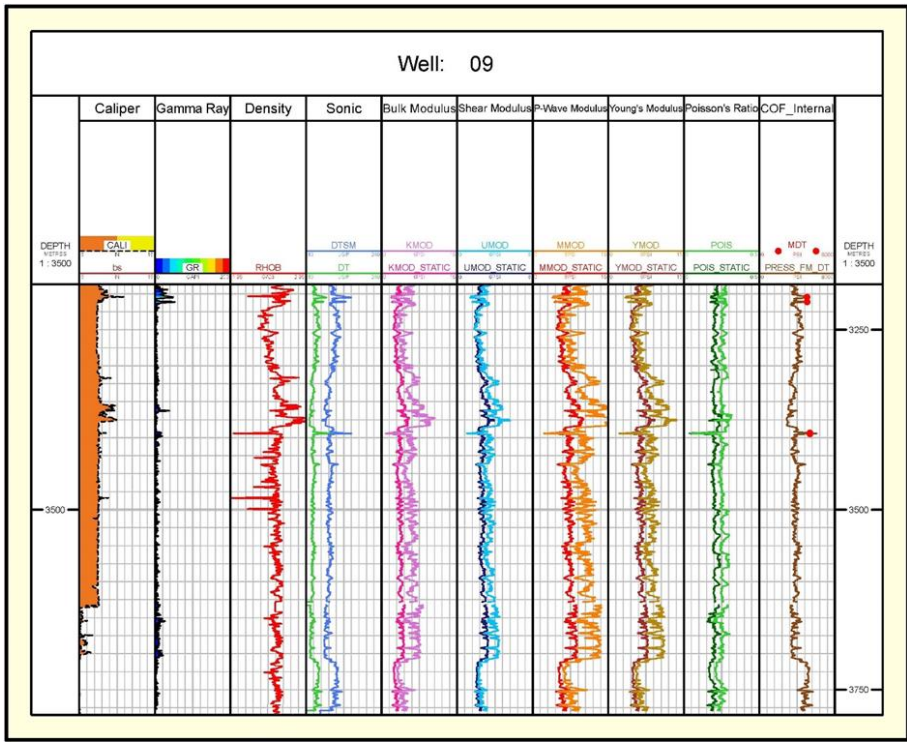

Figure3. Calculated geomechanical elastic parameters vs. depth (m)

2.3. Rock strength parameters

A uniaxial test is used to measure rock strength. There are several equations proposed to calculate UCS. A work by Asef *et al.* [14] (Eq.3) and Militzer and Stoll [15] (Eq.4) were used for estimating this parameter for carbonate reservoirs, and the results are shown in Figure 4 [15-16].

$$UCS = 2.65 * \left(\frac{Estatic^{0.8}}{\varphi^{0.2}}\right) \ldots\ldots \quad (3)$$

$$UCS = \left(\frac{7682}{\Delta t}\right)^{1.82} .145 \ldots\ldots. \quad (4)$$

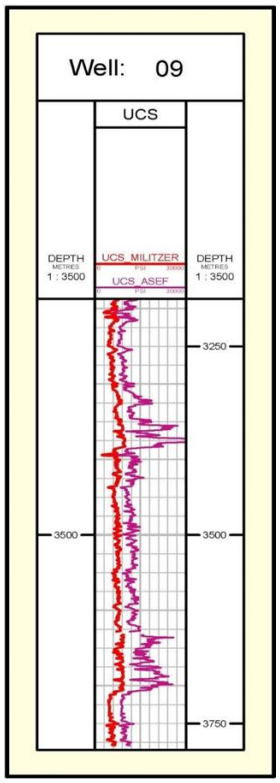

2.4. Pore pressure

The actual pore pressure values were obtained from carefully conducted and recorded flow checks, properly documented kicks, or pressure measurements using the RFT or MDT tool; they can be used to calibrate the pore pressure analysis from the offset log data [17]. Eaton's method relies on this assumption that overburden pressure is supported by pore pressure and effective vertical stress emanating from Terzaghi's equation (Eq.5) [18].

$$PPG = OBG - (OBG - HG) \times \left(\frac{\Delta t_{norm}}{\Delta t_{obs}}\right)^{x} \quad (5)$$

where PPG is the pore pressure gradient (psi.ft).

In this study, X is assumed 0.5 in the carbonate fields, and the hydrostatic gradient is assumed 10.5 kPa.m according to the overall studies in the Middle East, especially in Iran [19]. The MDT data were reported in intended well between 3204 m to 3394 m. The estimated Eaton`s pore pressure was calibrated with the MDT data.

Figure 4. Calculated uniaxial compressive strength (UCS) vs. Depth (m). The Red line is Militzer and Stoll [15], and the violet line is Asef [14]

2.5. In-situ horizontal stresses

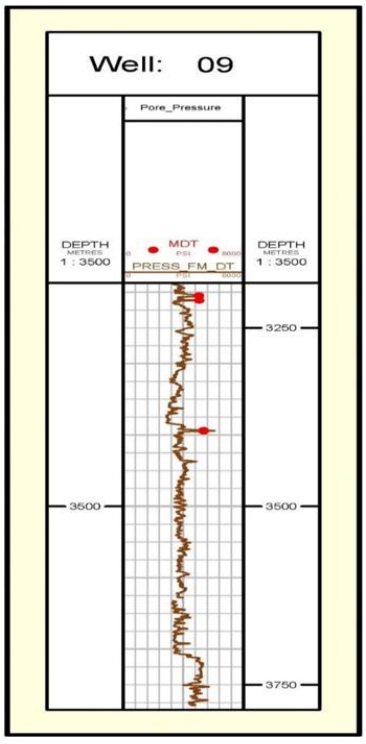

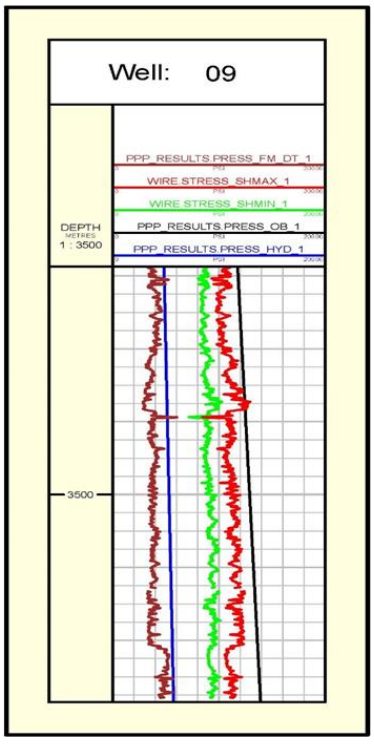

In an area with different faulting regimes, knowing the amount and direction of stresses can lead to a conscious decision. In homogeneous regions, the minimum and maximum horizontal stresses are the same. However, in the presence of fractures and faults, these values are affected by active tectonics and will not be the same anymore [20-21]. In this study, the poroelastic horizontal strain model was used to determine the magnitude of the minimum and the maximum horizontal stress. Figures 5a and 5b show the pore pressure calibration using MDT data and comparison of different stress profiles.

Figure 5a. Calibration of pore pressure with MDT data between 3200 to 3400 m

Figure 5b. Comparison of stress profile. The dark brown color is pore pressure; the Blue line is hydrostatic, the green line is min. hor. stress, the red line is max. hor. stress, and the black line is vertical stress

3. Mars Method

3.1. Artificial intelligence modeling

ANFIS method based on the Takagi–Sugeno fuzzy inference system with two types of clustering, including Fuzzy C-mean clustering and Subtractive clustering was used. In this study, porosity-neutron (NPHI), density (RHOB), sonic (DTs), and gamma-ray logs versus depth were utilized as a fuzzy-neural system input data for estimating Young's modulus, Poisson's Ratio, UCS, vertical overburden, and minimum and maximum horizontal stress as an output. Also, 70% of the data were used as training data and 30% as testing and evaluation data. It should be noted that the test data were not involved in the system training process.

3.2. ANFIS method with C-meaning clustering

The general structure of ANFIS for predicting the rock geomechanical properties is shown in Figure 6.

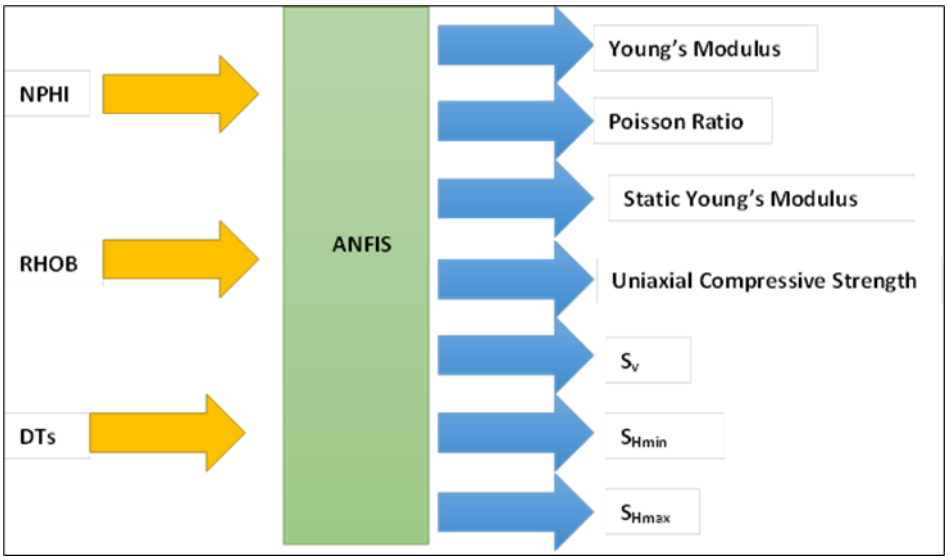

Figure 6. The general structure of ANFIS

Mean Square Error (MSE) and Coefficient of Determination were used for performance evaluation as given by Eq. 6.

$$MSE = \frac{\Sigma_{i=1}^{n\Sigma}\left(Y_i^{exp}{}_i^{per}\ ()^2\right)}{n} \quad (6)$$

where Y^{exp} and Y^{per} are experimental results and estimated value, respectively.
Table 1 shows the MSE for the various parameters for the optimized test data separately.

Table 1. Mean squared error for the geomechanical parameters

	Young modulus	Poisson's Ratio	Static Young modulus	UCS	Overburden Press	Min. Horizontal Stress	Max. Horizontal Stress
MSE	0.14	0.01	0.39	0.06	0.47	0.32	0.34

As can be seen from the results reported in the table, the highest estimation error is related to the uniaxial compressive strength parameter, and the least error belongs to the minimum Poisson's ratio. The system with C-clustering shows acceptable average performance in estimating the reservoir geomechanical parameters. The quality charts for the target data and the estimated data for the various parameters were plotted in Figures 7a to 7e. The coefficient of determination is expressed as an important parameter for evaluating system performance for each parameter.

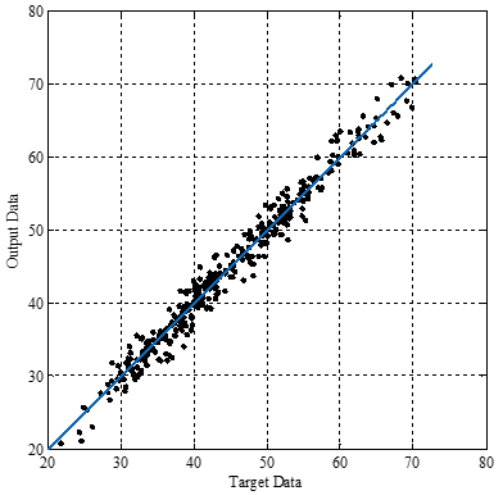

Figure 7a. Quality diagram related to Young's modulus (Gpa); R^2 = 0.9754

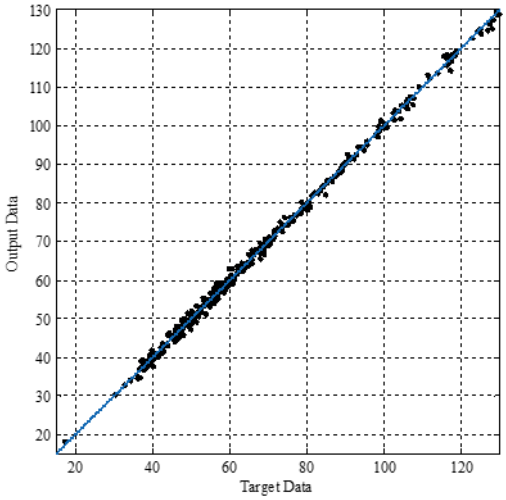

Figure 7b. Quality diagram related to UCS; R^2 = 0.9983

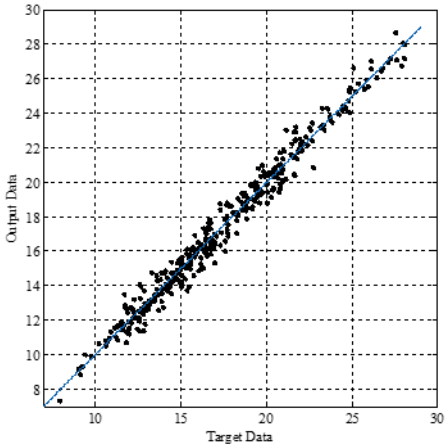

Figure 7c. Quality diagram related to Static Young modulus (Gpa); R^2 = 0.9780

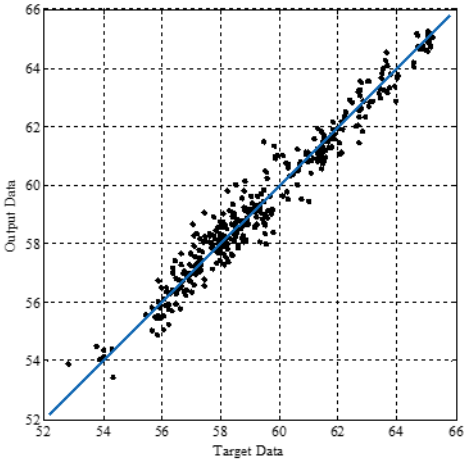

Figure 7d. Quality diagram related to Max. Horizontal Stress (Mpa); R^2=0.9532

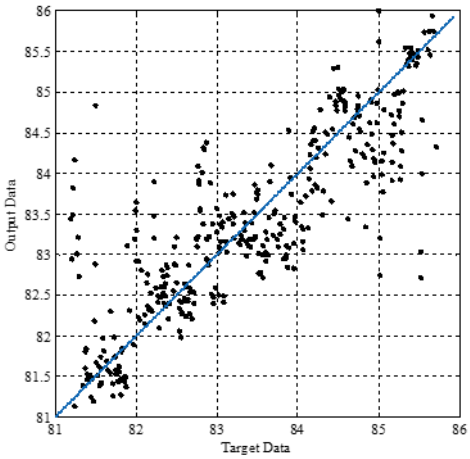

Figure 7e. Quality diagram related to Overburden Pressure (Mpa); R^2 = 0.6373

Although there are desirable correlation and regression values for Young's modulus, Poisson's Ratio, Static Young modulus, UCS in scatter plots, still it is not good enough as much as the other parameters for overburden pressure yet. Thus, the ANFIS method with subtractive clustering was employed in the section ahead. The fuzzy C means system results, and its comparison are given in Tables 2 and 3. Due to the random selection of test data, the data reported in the tables are not in in-depth order.

Table 2. Comparison between C-mean neural network outputs and target data for Young Modulus Poisson's Ratio and Static Young Modulus

Depth (m)	Young Modulus Target (Gpa)	Young Modulus Output (Gpa)	Poisson's Ratio Target	Poisson's Ratio Output	Static Young Modulus Target (Gpa)	Static Young Modulus Output (Gpa)
3368/99	56/64	57/28	0/32	0/32	22/42	22/20
3348/88	55/59	55/16	0/31	0/32	21/98	22/25
3369/75	53/16	53/18	0/31	0/31	20/97	20/75
3227/26	33/54	34/50	0/29	0/29	12/84	12/53
3189/77	47/32	46/34	0/31	0/30	18/56	18/42
3263/68	38/83	41/35	0/30	0/30	15/03	14/21
3360/46	68/32	70/81	0/32	0/32	27/26	27/24
3286/70	33/76	34/53	0/29	0/29	12/94	12/58
3345/37	48/23	48/64	0/31	0/31	18/93	19/07
3334/40	47/96	45/35	0/31	0/31	18/82	18/89
3197/39	53/56	53/70	0/31	0/31	21/14	23/07
3198/91	45/19	45/15	0/30	0/30	17/67	18/71
3276/64	36/81	34/83	0/30	0/29	14/20	14/47
3190/08	45/21	44/66	0/30	0/31	17/68	18/79
3223/76	31/28	32/38	0/29	0/29	11/91	11/21
3297/36	42/57	43/84	0/30	0/30	16/59	17/27
3322/21	62/44	62/93	0/32	0/32	24/82	24/09
3209/58	49/63	53/41	0/31	0/31	19/51	20/80
3247/53	28/17	27/89	0/28	0/29	10/62	10/53
3294/32	32/56	30/37	0/29	0/29	12/44	11/50
3312/76	52/08	53/31	0/31	0/31	20/53	20/38
3311/23	51/75	52/05	0/31	0/31	20/39	19/62
3221/01	37/96	39/54	0/30	0/30	14/68	14/44
3323/43	54/90	54/08	0/32	0/31	21/70	22/45
3233/81	34/59	33/30	0/29	0/29	13/28	14/78
3353/14	54/77	51/91	0/31	0/32	21/64	21/53
3308/64	46/07	46/37	0/31	0/31	18/04	18/22
3239/45	36/78	34/83	0/30	0/30	14/18	13/78
3367/16	64/92	65/40	0/32	0/33	25/85	25/94
3274/66	36/03	36/28	0/29	0/30	13/88	14/76
3319/62	54/21	54/11	0/31	0/31	21/41	21/62
3234/73	35/63	35/28	0/29	0/29	13/71	12/60
3257/13	43/48	44/07	0/30	0/30	16/97	16/98
3363/20	55/55	54/71	0/32	0/32	21/97	21/87

As shown in Table 2, the estimated values are very close to the target values, which confirms the accuracy of the C-mean method in estimating the desired parameters.

Table 3 compares the estimated performances of uniaxial compressive strength parameters, vertical stress, minimum horizontal stress, and maximum horizontal stress with target values. The outputs show that the results are very close to the target values, and the C-mean neural system results good average accuracy.

Table 3. Comparison between C-mean neural network outputs and target data for UCS, vertical stress, Min. Hor. Stress, and Max. Hor. Stress

Depth (m)	UCS Target (Mpa)	UCS Output (Mpa)	Vertical Stress Target (Mpa)	Vertical Stress Output (Mpa)	Min. Hor. Stress Target (Mpa)	Min. Hor. Stress Output (Mpa)	Max. Hor. Stress Target (Mpa)	Max. Hor. Stress Output (Mpa)
3368/99	98/30	97/05	85/68	86/32	62/60	61/92	63/45	63/66
3348/88	102/45	102/07	85/16	84/14	61/88	61/47	62/72	62/35
3369/75	114/00	113/83	85/70	84/33	61/96	60/70	62/76	63/53
3227/26	47/88	48/15	82/18	82/53	55/95	56/26	56/45	57/45
3189/77	72/92	72/97	81/24	84/17	57/80	59/87	58/51	60/04
3263/68	50/52	51/49	83/05	83/16	57/59	57/64	58/17	57/91
3360/46	125/17	123/81	85/46	85/36	64/00	63/18	65/03	64/90
3286/70	45/78	44/03	83/60	83/02	56/94	56/79	57/45	56/78
3345/37	74/50	74/45	85/07	84/79	60/70	60/64	61/42	60/56
3334/40	78/34	77/39	84/79	84/25	60/42	59/86	61/14	60/92
3197/39	95/72	95/99	81/43	81/51	58/78	58/55	59/58	60/26
3198/91	64/61	64/44	81/47	81/20	57/42	58/05	58/10	58/30
3276/64	54/43	54/01	83/36	82/98	57/44	57/10	57/98	57/44
3190/08	67/97	67/12	81/24	81/14	57/41	57/71	58/09	57/93
3223/76	45/96	45/85	82/10	82/27	55/49	56/32	55/95	55/93

3.3. ANFIS method with subtractive clustering

In this section, the performance of the neuro-fuzzy system was investigated based on clustering. The impact radius of the subtractive clustering factor was analyzed as an influencing factor in the system's performance and accuracy. As Figure 8 shows, the lowest total estimation error is when the impact radius of the system is 0.15. In this case, the mean square error is 0.6977. Therefore, it can be concluded that the optimal impact radius for each dataset must be found, and having a low or high impact radius does not necessarily mean the more desirable accuracy of the system.

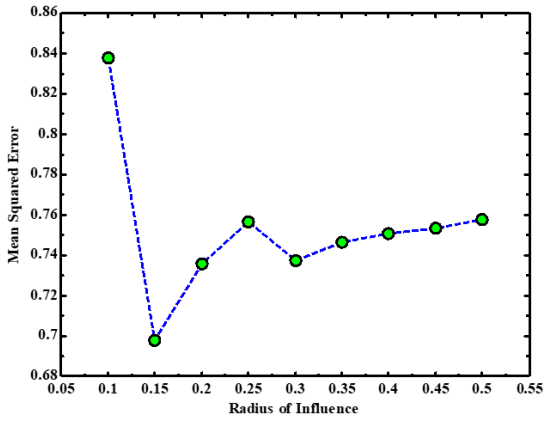

Figure 8. Impact radius effect on prediction accuracy of Subtractive neuro-fuzzy system

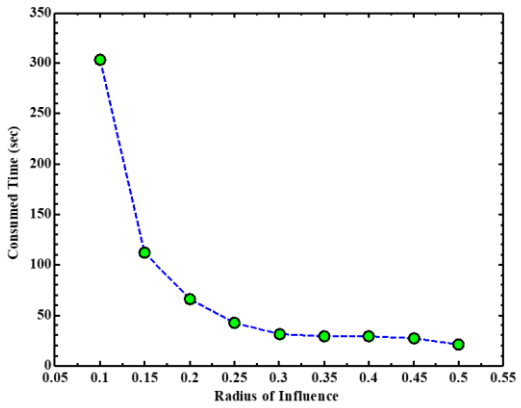

Figure 9. The time required for predicting the geomechanical parameters by the subtractive neuro-fuzzy system in terms of the impact cluster radius

Table 4 shows the performance of the subtractive neuro-fuzzy system in estimating different geomechanical parameters.

Table 4. Subtractive neuro-fuzzy system for predicting different geomechanical parameters

	Young modulus	Poisson's Ratio	Static Young modulus	UCS	Overburden Press.	Min. Horizontal Stress	Max. Horizontal Stress
MSE	0.13	0.00	0.37	0.22	0.47	0.34	0.36

The least error value achieved for Poisson's ratio, nearly 0, while overburden pressure has the most value of 0.47.

Figure 9 illustrates the time changes required to complete the estimation process in terms of the impact radius of the clustering method. Based on this figure, the greater the impact radius, the faster the estimation process.

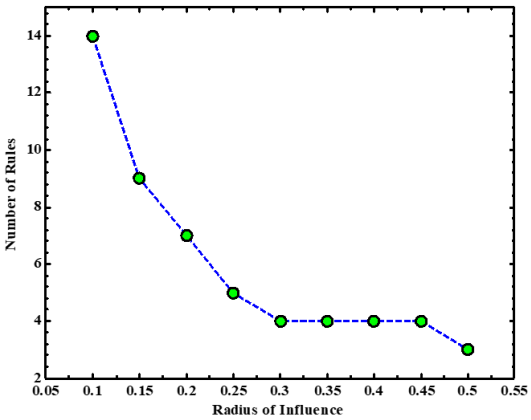

Figure 10. Changing the number of fuzzy system rules (clusters) in terms of the impact radius

Also, the radius of impact can change the number of fuzzy rules or, in other terms, the number of clusters used in the estimation operation. Figure 10 shows that by changing the impact radius from 0.1 to 0.5, the number of fuzzy inference systems rules in the neuro-fuzzy system decreases from 14 to 3. Figure 11 shows the structure of the neuro-fuzzy system for estimating the Young's modulus parameter with the impact radius of 0.1 and 14 set rules, which were determined by the neuro-fuzzy system.

The fuzzy interface system with 14 rules for estimation of Young's modulus is presented in Figure 11, in which NPHI, RHOB, and DT versus depth feed as the main inputs of the model.

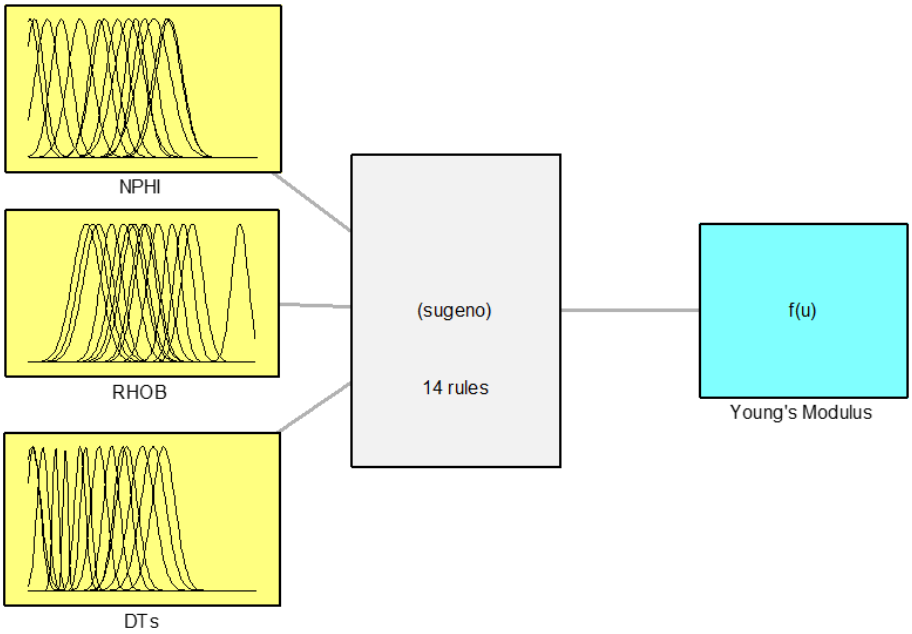

Figure 11. The fuzzy inference system's structure lies in the neural-fuzzy system for predicting Young's modulus when the number of fuzzy system rules is 14

4. Results and discussion

The trained ANFIS model was used to estimate geomechanical parameters. The training and test data, actual and estimated geomechanical properties versus depth are shown in Figure 12. Blue and red lines stand for target and output, respectively. The trends present a perfect match between target and output data, which proves the efficiency of the ANFIS model for estimating rock mechanic parameters, as demonstrated in Figure 12. Overall, it can be seen that the ANFIS model can accurately estimate the geomechanical parameters very fast.

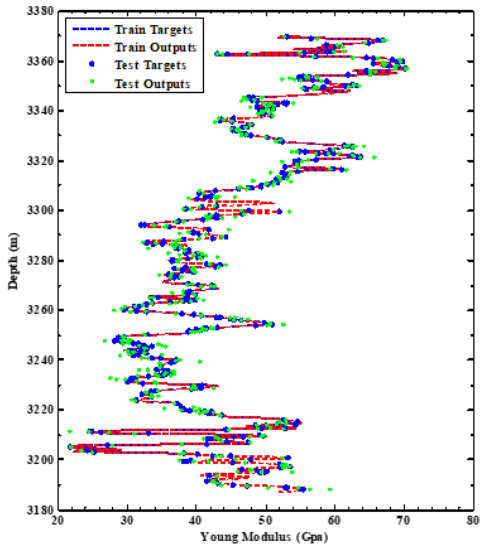
Train Targets
Train Outputs
Test Targets
Test Outputs
Depth (m)
Young Modulus (Gpa)

(a)

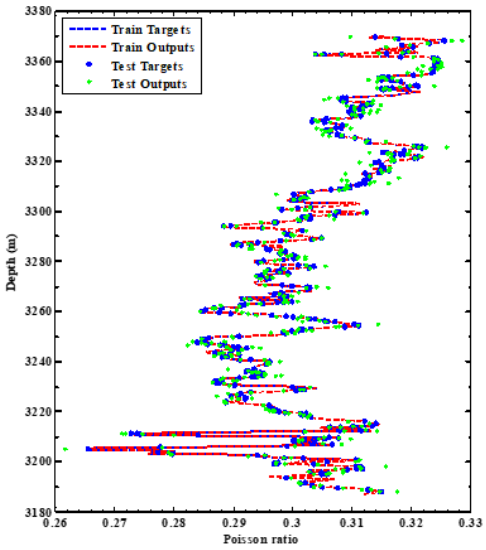
Train Targets
Train Outputs
Test Targets
Test Outputs
Depth (m)
Poisson ratio

(b)

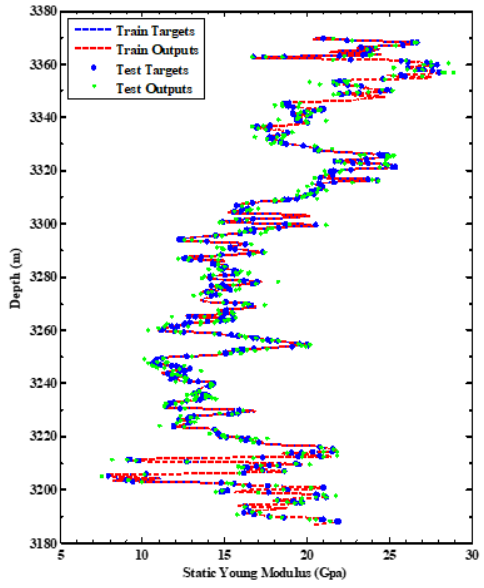
Train Targets
Train Outputs
Test Targets
Test Outputs
Depth (m)
Static Young Modulus (Gpa)

(c)

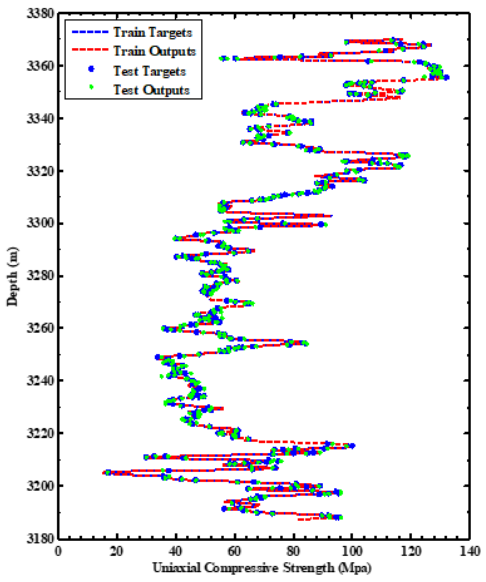
Train Targets
Train Outputs
Test Targets
Test Outputs
Depth (m)
Uniaxial Compressive Strength (Mpa)

(d)

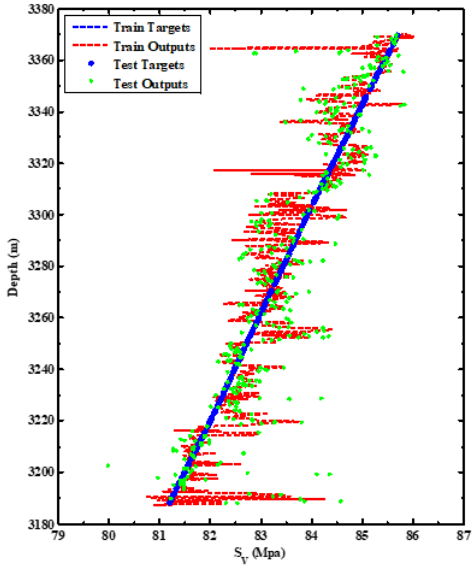
Train Targets
Train Outputs
Test Targets
Test Outputs
Depth (m)
S_V (Mpa)

(e)

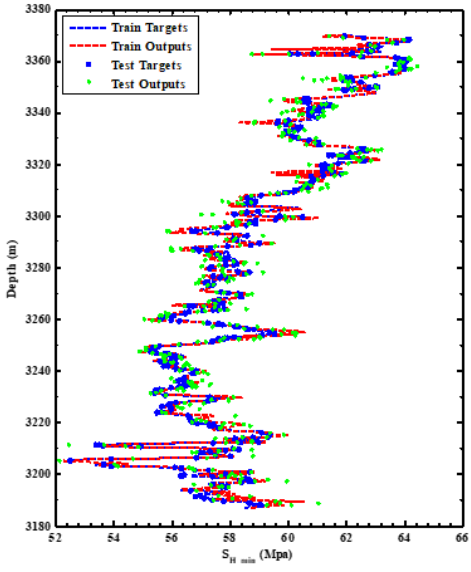
Train Targets
Train Outputs
Test Targets
Test Outputs
Depth (m)
S_H min (Mpa)

(f)

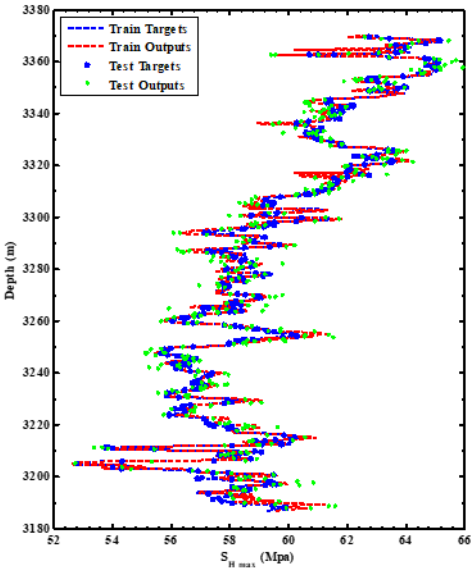

(g)

Figure 12. ANFIS output for rock mechanic parameters and stress magnitude

Based on the results in the C-mean neuro-fuzzy system, R-squared for the vertical stress was lower than the other parameters. This phenomenon was repeated in this section. It is probably due to the sensitivity of the vertical stress to the depth, and it is the crucial missing parameter in the inputs of the neuro-fuzzy system. Thus, we decided to develop and evaluate a new neuro-fuzzy system in the presence of the depth selected as input to improve estimation of this parameter.

The result of this evaluation was positive, and Figure 13 shows the obtained quality chart. Figure 14 shows the vertical stress diagram versus depth with the modified method. According to these graphs, the improvement of the estimation of this parameter is noticeable.

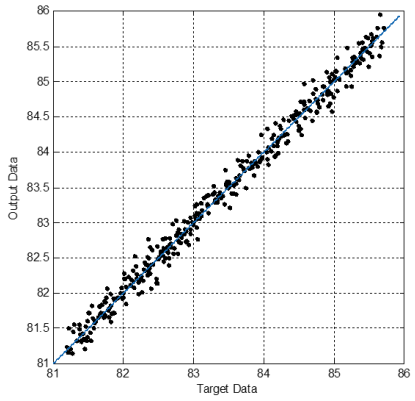

Figure 13. Optimized vertical stress quality chart with R^2=0.998

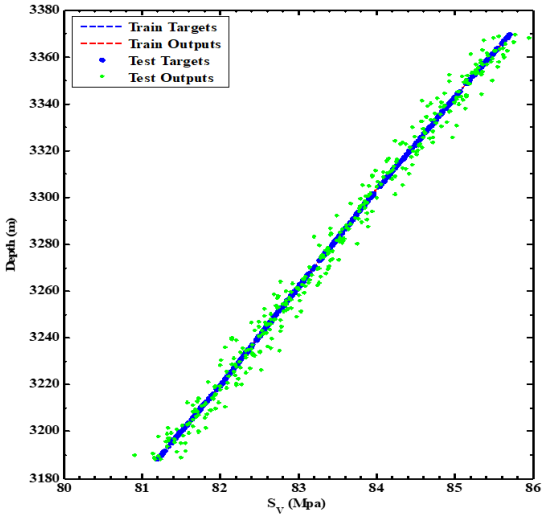

Figure 14. Vertical stress variations vs. depth and improvement of neuro-fuzzy system performance in prediction

The estimation was improved by the modified model, and it can be argued variation of stress with depth is more sensitive in respect to changing formation type along with well. The linear regression of the outputs and the corresponding target of the neuro-fuzzy system

performance in estimating vertical stress variations versus depth that provide good correlation and regression values is shown in Figure 14.

4.1. Comparison of the Neuro-Fuzzy Systems methods

In this section, the performances of the two neuro-fuzzy systems used in this study were compared. As can be seen in Tables 5 and 6, there are slights differences between the performances of the two systems, and both systems are well enough to estimate the geomechanical parameters. The time required to complete the estimation process was 115 seconds for the subtractive neuro-fuzzy system and 175 seconds for the C-mean system.

Table 5. Comparison of the two Neuro-Fuzzy Systems (Section I)

	Young's modulus		Poisson's Ratio		Static Young modulus	
	C-mean	subtractive	C-mean	subtractive	C-mean	subtractive
MSE	0.14	0.13	0.00	0.00	0.39	0.37
R^2	0.9754	0.9800	0.9717	0.9712	0.9780	0.9812

For Young and static Young modules, the neuro-fuzzy system with subtractive clustering is a little more accurate than the C-mean clustering, while there are about the same for Poisson's ratio.

Table 6. Comparison of the two Neuro-Fuzzy Systems (Section II)

	UCS		Vertical Stress		Min. Hor. Stress		Max. Hor. Stress	
	C-mean	subtractive	C-mean	subtractive	C-mean	subtractive	C-mean	subtractive
MSE	0.06	0.22	0.47	0.47	0.32	0.34	0.34	0.36
R^2	0.9983	0.9980	0.6373	0.6521	0.9438	0.9438	0.9532	0.9441

For UCS, minimum and maximum horizontal stresses, both of the methods almost provide comparable and sufficient results, but none of them can estimate the outputs or close value to the corresponding target, say about 0.63 and 0.65, which are too far from the other results.

The data-driven model performance compared here confirms the efficiency of the ANFIS method as a reliable tool for the geomechanical properties. Overall, the ANFIS models obtain R^2 over 90% in both subtractive and C-mean clustering.

5. Conclusions

A method to estimate the geomechanical parameters based on machine learning technique (ANFIS) using well logging data was introduced in this work. First, a borehole geomechanical model was developed for an oil well in an Iranian oil field. The dynamic rock mechanical data from different lithologies were calculated and converted to static elastic parameters by conventional equations. Pore pressure was estimated based on the Eaton method and calibrated by MDT data, which were recorded between 3204 m to 3394 m. Vertical stress was calculated based on the density of the layers and minimum, and maximum horizontal stresses were determined based on poroelastic horizontal strain. Next, determining the geomechanical parameters based on Takagi-Sogno neuro-fuzzy systems provided more accurate results than conventional methods. However, there are slight differences between the accuracy of these two approaches. It is perceived that the Poisson ratio is more accurate, and the vertical stress is associated with a higher error due to the sensitivity to the depth.

Moreover, using depth as one of the inputs can significantly increase the accuracy of the results. Furthermore, it is identified that the C-clustering algorithm completes the estimation process more rapidly. Moreover, the results show that a normal fault regime can be seen in the field, which agrees with the real data. Based on the model output, low pore pressure can be observed in this well, which may have led to several challenges.

Nomenclature

OBG	*overburden gradient (psi.ft)*
HG	*hydrostatic gradient (psi.ft). 10.5 kPa.m according to the overall studies in the Middle East, especially in Iran (Atashbari et al. 2015)*
Δt_{norm}	*normal sonic log value (us.ft)*
Δt_{obs}	*observed sonic log value (us.ft)*
X	*exponent value, which is dependent on formation properties.*

References

[1] Widrow B, Rumelhar, DE, and Lehr MA. Neural Networks: Applications in Industry, Business and Science. Communications of the ACM, 1994; 37: 93-105.

[2] Sharda R. Neural Networks for the MS.OR Analyst: An Application Bibliography. Interfaces, 1994; 24(2), 116-130. Retrieved January 19, 2021, from http:..www.jstor.org.stable.25061866 Wong PM, and Nikravesh M. Field applications of intelligent computing techniques: Journal of petroleum geology, 2001; 24(4): 381-387.

[3] Fattahpour V, Pirayegar A, Dusseault MB, Mehrgini B. Building a mechanical earth model: a reservoir in southwest Iran. Selected as a presentation at the 46th symposium of US rock mechanics. geomechanics by an ARMA technical program committee held in Chicago, IL, USA, 24-27 June 2012. 12-404.

[4] Silpngarmles N, Guler B, Ertekin T, and Grader AS. Development and testing of two-phase relative permeability prediction using artificial neural networks: SPE 2002, 79547: 299-308

[5] Sayers CM, and den Boer LD. Pore-Pressure Prediction in the Permian Basin Using Seismic Prestack Inversion. Unconventional Resources Technology Conference, 2170-2180. Society of Petroleum Engineers 2019, Denver, Colorado, USA.

[6] Herwanger J, Koutsabeloulis N. Seismic Geomechanics How to Build and Calibrate Geomechanical Models using 3D and 4D Seismic Data; EAGE Publications, 2011, ISBN 978-90-73834-10-1.

[7] Atashbari V, Tingay M. Pore pressure prediction in carbonate reservoirs. SPE Latin American and Caribbean Engineering Conference 2012; 150835.

[8] Hottmann CE, Johnson RK. Estimation of formation pressure from log derive shale properties. J. Pet Technol., 1965; 17(6): 717-722.

[9] Azadpour MN, Manaman S, Kadkhodaei-Ilkhchi A, Sedighpor M. Pore pressure prediction and modeling using well-logging data in one of the gas fields in south of Iran. Journal of Petroleum Science and Engineering, 2015; 128: 15-23.

[10] Alsiyabi K, Al-Aamri M, Siddiqui N. Effective Geomechanic Approach for Wellbore Stability Analysis; SPE Middle East Oil and Gas Conference held in Manama, Bahrain 2019, SPE-194922-MS.

[11] Knoll L. The process of building a mechanical earth model using well data (Master Thesis), Montan University 2016, Austria.

[12] Greenberg ML, and Castagna JP. Shear-wave estimation in porous rocks: Theoretical formulation, preliminary verification, and applications: Geophysical Prospecting, 1992; 40(2): 195–209.

[13] Bradford IDR, Fuller J, Thompson PJ, Walsgrove TR. Benefits of assessing the solids production risk in a North Sea reservoir using elastoplastic modelling (SPE.ISRM 47360).

[14] Asef MR, and Farrokhrouz M. Methods and parameters for estimation of wave velocity in rock. In: 19th Int. Geophysical Congress and Exhibition, 23-26 November 2010, Turkey, Ankara.

[15] Militzer H, Stoll R. 1973. "Einige Beitraegeder Geophysik zur primaerdatenerfassung im Bergbau," Neue Bergbautechnik, Leipzig, Vol. 3, No. 1, pp 21–25.

[16] Guerra C, Fischer K and Henk A. Stress prediction using 1D and 3D geomechanical models of a tight gas reservoir—A case study from the Lower Magdalena Valley Basin, Colombia. Geomechanics for Energy and the Environment, 2019; 19, 100113.

[17] Eaton BA. (1975). "The equation for geopressure prediction form wells logs." SPE, 5544. FOSTER, J. B. & WHALEN, H. E.

[18] Atashbari V, Tingay M, and Amrouch K. Overpressure in the Abadan Plain, Iran. International Conference and Exhibition, Melbourne, Australia 13-16 September 2015;. ISSN (online):2159-6832, Pages: 564.

[19] Gholamia R, Moradzadeha A, Rasoulib V, Hanachic J. Practical application of failure criteria in determining safe mud weight windows in drilling operations. Journal of Rock Mechanics and Geotechnical Engineering , 2014 ;6: 13–25.

[21] Fjaer E, Holt RM, Horsrud P, and Raaen AM. Petroleum related rock mechanics (2nd edition). Elsevier Publishing 2008, 135-175.
[21] Obimma KJ, Obiora DN, Oha AI, Ibuot JC, Yakubu JA. Seismic and Petrophysical Characterization of Reservoirs in Kjoe Field, On-Shore Niger Delta, Nigeria, 2021, Pet Coal, 63 (1): 50-62.

To whom correspondence should be addressed: Professor Amir H. Mohammadi, Discipline of Chemical Engineering, School of Engineering, University of KwaZulu-Natal, Howard College Campus, King George V Avenue, Durban 4041, South Africa, E-mail: amir_h_mohammadi@yahoo.com